Post-Print

This is the accepted version of:

A. Romero-Calvo, A.J. Garcia-Salcedo, F. Garrone, I. Rivoalen, F. Maggi
Lateral and Axisymmetric Ferrofluid Oscillations in a Cylindrical Tank in Microgravity
AIAA Journal, Vol. 60, N. 4, 2022, p. 2707-2712
doi:10.2514/1.J061351

The final version of this paper can be found in https://doi.org/10.2514/1.J061351

Lateral and axisymmetric ferrofluid oscillations in a cylindrical tank in microgravity

Álvaro Romero-Calvo *
Department of Aerospace Engineering Sciences, University of Colorado Boulder, Boulder, CO, United States

Antonio J. García-Salcedo†, Francesco Garrone‡, Inés Rivoalen§, and Filippo Maggi¶
Department of Aerospace Science and Technology, Politecnico di Milano, Milan, Italy

I. Introduction

Magnetic polarization forces are becoming increasingly popular in space technology as a means of controlling multiphase flows in reduced gravity environments. Applications include mass transfer [1–5], spacecraft propulsion [6–8], thermomagnetic convection [9, 10], phase separation [11], sample holding [12], or diamagnetically-enhanced electrolysis [13], among others. The polarization force can be induced on natural liquids and magnetically-enhanced substances, which are classified as diamagnetic, paramagnetic, or ferromagnetic. Although the dia/paramagnetic force is so weak that terrestrial applications are almost nonexistent, in microgravity even the slightest disturbance can determine the behavior of a fluid system [14]. The same force acting on a highly-susceptible ferrofluid can be dominant both on Earth and in space [15].

The simulation of low-gravity multiphase flows subject to inhomogeneous polarization forces is severely complicated by the coupling between fluid and magnetic problems and the presence of strong capillary forces [16]. However, some of the most important space applications can still be addressed by means of efficient quasi-analytical tools. Following the track of classical low-gravity fluid mechanics research [17, 18], recent works have focused on the study of the equilibrium, stability, and free surface oscillations of inviscid magnetic liquid interfaces [19]. The latter is of particular importance for the development of novel magnetic liquid sloshing control devices, which have been recently proposed to complement or substitute traditional capillary propellant management devices [16]. The final goal of such systems is to transform a highly unpredictable propellant sloshing problem into a simple and reliable superposition of analogous linear oscillators.

Even though low-gravity liquid sloshing and its interactions with spacecraft dynamics continue to be very active fields of research [20–26] and a number of publications have explored the magnetic positioning of liquid oxygen and low-susceptibility ferrofluids in microgravity [27–35], the study of highly susceptible ferrofluids for space applications

*Graduate Research Assistant, Department of Aerospace Engineering Sciences, University of Colorado Boulder, alvaro.romerocalvo@colorado.edu, AIAA Student Member.
†Graduated student, Department of Aerospace Science and Technology, Politecnico di Milano.
‡Graduated student, Department of Aerospace Science and Technology, Politecnico di Milano.
§Graduated student, Department of Aerospace Science and Technology, Politecnico di Milano.
¶Associate Professor, Department of Aerospace Science and Technology, Politecnico di Milano, AIAA Senior Member.

The final version of this paper can be found in https://doi.org/10.2514/1.J061351

is still in its infancy. The accurate determination of the modal shapes and frequencies of oscillating ferrofluid surfaces in low-gravity is, however, critical for magnetic sloshing control devices. In order to cover this fundamental gap, the European Space Agency (ESA) *Drop Your Thesis!* 2017 [36, 37] experiment studied the axisymmetric oscillations of water-based ferrofluids in cylindrical tanks when subjected to an inhomogeneous magnetic field in microgravity. The results show that the theoretical model presented in Ref. 19 overestimates the axisymmetric magnetic frequency response, pointing to the existence of unaccounted physical effects such as viscous damping or a complex magnetic influence on the contact line hysteresis process [38]. Lateral oscillations, which have an intrinsic technical value as main sources of attitude disturbances, remained unexplored. The United Nations Office for Outer Space Affairs (UNOOSA) *DropTES* 2019 StELIUM experiment, whose design is described in Refs. [39–41], was subsequently launched at the drop tower of the Center of Applied Space Technology and Microgravity (ZARM) to complement the analysis initiated in Ref. 38 with the lateral sloshing case.

This technical note presents the final results of the UNOOSA *DropTES* 2019 StELIUM experiment and addresses the influence of the magnetic field generated by a circular coil on the fundamental axisymmetric and lateral frequencies of an oscillating ferrofluid located in a cylindrical tank in microgravity. Predictions from the aforementioned quasi-analytical free surface oscillations model are compared with the experiments under different regimes. The framework of analysis introduced in Ref. 19 is summarized in Sec. II, followed by a description of the experimental methods in Sec. III and the discussion of results in Sec IV.

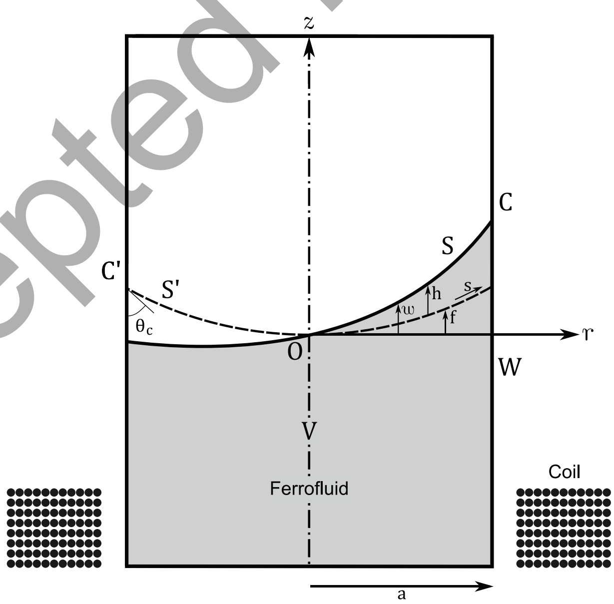

Fig. 1 Geometry of the system under study.

The final version of this paper can be found in https://doi.org/10.2514/1.J061351

II. Magnetic free surface oscillations model

The system under study, represented in Fig. 1, consists of an upright cylindrical tank with radius a that contains a volume V of a water-based ferrofluid in microgravity. The liquid is incompressible and Newtonian, and has density ρ, surface tension σ, and static wall contact angle θ_c. The free space is filled by air at pressure p_g. In microgravity, a coil located at the base of the vessel generates an inhomogeneous axisymmetric magnetic field $\boldsymbol{H}$ that interacts with the magnetic fluid with magnetization $M(H)$, with H and M being the modules of their corresponding vector fields. In Fig. 1, s is a curvilinear coordinate along the meniscus with origin in the vertex O, and the local vertical coordinates are given by w (fluid surface - vertex), f (meniscus - vertex) and h (fluid surface - meniscus). The dynamic (S) and static (S') fluid surfaces meet the wall W of the vessel at the contact lines C and C', respectively. The set of cylindrical coordinates $\{r, \theta, z\}$, centered at the vertex of the meniscus, is considered in the analysis.

The oscillations of free liquid surfaces in microgravity have traditionally been studied through modal analysis [42, 43] and then validated using microgravity experiments [44–52] already since the development of the first non-magnetic low-gravity free surface oscillation model by Satterlee and Reynolds in 1964 [53]. One of the main reasons for adopting this approach is the complete analogy between the modal decomposition process and the superposition of linear spring-mass-damper systems employed to model liquid sloshing [14, 18, 54, 55]. The framework here presented for magnetic liquids, summarized from Ref. 19, is not an exception. It assumes an inviscid, potential, isothermal, and magnetically dilluted flow to which the ferrohydrodynamic Bernoulli equation [56] is applied. After linearizing the equations of motion around the meniscus, the variational principle

$$
\begin{aligned}
J = \iint_{S'} \Bigg[& \frac{\mathcal{H}_R^2}{\left(1+F_R^2\right)^{3/2}} + \frac{1}{R^2}\frac{\mathcal{H}_\theta^2}{\left(1+F_R^2\right)^{1/2}} \\
& + \left(Bo + Bo_{\text{mag}}(R)\right)\mathcal{H}^2 - \Omega^2\Phi\mathcal{H}\Bigg] R dR d\theta - \Omega^2 \iint_W \Phi G R dR d\theta - \Gamma \int_{C'} \left[\frac{\mathcal{H}^2}{\left(1+F_R^2\right)^{3/2}}\right]_{R=1} \mathrm{d}\theta \\
= \text{extremum} &
\end{aligned} \tag{1a}
$$

is obtained, subjected to

$$\nabla^2\Phi = 0 \text{ in } V, \tag{1b}$$

$$\mathcal{H} = \Phi_Z - F_R\Phi_R \text{ on } S', \tag{1c}$$

$$G = \Phi_Z - W_R\Phi_R \text{ on } W, \tag{1d}$$

$$\mathcal{H}_R = \Gamma\mathcal{H} \text{ on } C', \tag{1e}$$

The final version of this paper can be found in https://doi.org/10.2514/1.J061351

where the subindices denote the partial derivatives. The magnetic Bond number is defined as

$$Bo_{\mathrm{mag}}(R) = -\frac{\mu_0 a^2}{\sigma}\left(M\frac{\partial H}{\partial z} + \mathrm{M}_n\frac{\partial \mathrm{M}_n}{\partial z}\right)_{F(R)}, \tag{2}$$

and describes the ratio between magnetic and surface tension forces. The dimensionless cylindrical coordinates $R = r/a$, $Z = z/a$, vertical coordinates $F = f/a$, $\phi(R,\theta,Z,t) = \sqrt{g_0 a^3}\Phi(R,\theta,Z)\sin(\omega t)$, $h(R,\theta,t) = \sqrt{a g_0/\omega^2}\mathcal{H}(R,\theta)\cos(\omega t)$, circular frequency $\Omega^2 = \rho a^3\omega^2/\sigma$, and hysteresis parameter $\Gamma = a\gamma$ are employed with $g_0 = 9.81\ m/s^2$ being the gravitational acceleration at ground level, ϕ the dimensional perturbed velocity potential, and ω the dimensional circular frequency. G is a function defined by Eq. 1d that accounts for the non-penetration wall boundary condition and that arises naturally after reducing a volume integral in the original form of Eq. 1a to a surface integral using Green's theorem, as described in Ref. 43. The hysteresis parameter Γ in Eq. 1e can be regarded as the dynamic equivalent of the static contact angle θ_c, and describes how the dynamic surface interacts with the walls of the container. The limiting cases $\Gamma = 0$ and $\Gamma \to \infty$ lead to the *free-edge* and *stuck-edge* conditions, respectively. In other words, Γ describes how freely the contact line C slides over the walls of the tank, and has consequently a large influence on the shape of the eigenmodes and their associated eigenfrequencies [38].

The system described by Eqs. 1a-e is solved in two steps. First, the axisymmetric meniscus $F(R)$ is computed with an iterative algorithm that accounts for the fluid-magnetic coupling. The algorithm solves the meniscus balance equations (derived in Ref. 19) for a given magnetic field, and then the magnetic field is recomputed in Comsol Multiphysics employing the new interface. The process is repeated until the vertex of the meniscus converges with an error of ±0.1 mm. In a second step, Eqs. 1a-e are transformed into an eigenvalue problem by using Ritz's method with a set of admissible functions that enforce the boundary conditions given by Eqs. 1b-e. The process relies on the previously computed axisymmetric meniscus $F(R)$ and $Bo_{\mathrm{mag}}(R)$ number, and takes the geometry and magnetic environment, the physical properties of the liquid (ρ, σ, $M(H)$), and the wall boundary conditions (θ_c, Γ) as inputs. The solution of the eigenvalue problem is the eigenvalue ω_n and eigenmode $h^{(n)}$ for the axisymmetric or lateral mode n. Further details on the formulation and operation of this method can be found in Ref. 19. Its implementation is fully equivalent (excluding liquid and geometrical properties) to that described in Ref. 38.

III. Materials and methods

A. Experimental setup

The experimental setup of StELIUM, depicted in Fig. 2, is designed to operate in a 9.3 s catapult launch at ZARM's drop tower [57]. The system, that is thoroughly described in Ref. 39, is subdivided into two identical assemblies that contain a cylindrical Plexiglas container, a surrounding electromagnetic coil, and an horizontal linear slider that imposes a lateral oscillation to the fluid in the middle of the flight. This oscillation induces a lateral sloshing wave that is

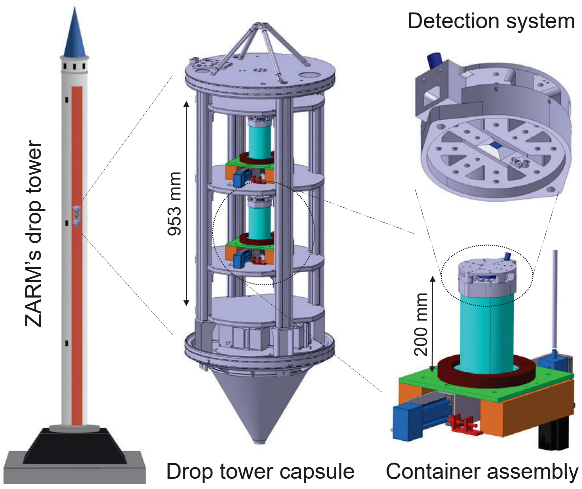

Fig. 2 Experimental setup (not in scale).

complemented with the axisymmetric wave induced by the initial launch acceleration. A restoring polarization force is applied to the ferrofluid during this process by operating the coils with constant current intensities I ranging from 0 to 20 A. The 20 A level generates an inhomogeneous magnetic force distribution with characteristic meniscus magnetic Bond number and accelerations values of ~ 35 and ~ 0.71 m/s^2, respectively.

The evolution of the free surface is captured by a custom device located on top of each container. A laser line is pointed at the surface of the ferrofluid while a camera records its projection. The deformation of the line is then correlated with the height of the surface, and the 3D liquid surface profile is extracted. The system is able to compute the axisymmetric meniscus, from which the apparent contact angles θ_c are derived, and the evolution of the axisymmetric and lateral waves along the direction of excitation. A modal projection is subsequently applied to compute the hysteresis parameter Γ from the lateral waves, while a Fast Fourier Transform of the movement of the laser line is employed to extract the modal frequencies. Γ is here assumed to be the same for axisymmetric and lateral modes. This assumption is motivated by the difficulty in extracting Γ in the axisymmetric case, where magnetic and non-magnetic modal shapes are very similar [38]. Further details on the design and operation of the detection system can be found in Refs. [40, 41].

B. Liquid properties

The liquid tank has 11 cm diameter and 20 cm height, and is filled up by a 1:5 volume solution of the Ferrotec EMG-700 water-based ferrofluid. Oil-based options are discarded to avoid the visualization issues reported in previous works [27]. The ferrofluid has a density of 1058 kg/m^3, surface tension of 55.6 mN/m, a viscosity of 1.448 mPa·s, employs an anionic surfactant, and contains a 1.16% vol concentration of 10 nm magnetic nanoparticles. The magnetization curve of the solution, that determines its magnetic response, was measured with a MicroSense EZ-9 Vibrating Sample Magnetometer, resulting in an initial magnetic susceptibility χ = 0.39 and saturation magnetization

The final version of this paper can be found in https://doi.org/10.2514/1.J061351

Table 1 Experimental results for contact angle, fundamental oscillation frequency and damping ratios for axisymmetric and lateral waves, and lateral hysteresis parameter

	I [A]	θ_c [deg]	Γ [-]	$\omega_{a,1}$ [rad/s]	$\xi_{a,1}$ [-]	$\omega_{l,1}$ [rad/s]	$\xi_{l,1}$ [-]
Upper	0	60.52	16.75	4.52	0.19	2.58	0.21
	10	59.87	7.23	5.82	0.15	3.62	0.16
	15	62.36	7.11	7.05	0.14	4.60	0.12
	20	65.67	4.41	7.60	0.13	5.30	0.11
Lower	0	47.52	15.27	3.62	0.23	2.21	0.22
	10	53.07	4.88	5.41	0.16	3.36	0.17
	15	58.15	5.44	5.98	0.17	4.18	0.15
	20	*	*	*	*	*4.90*	*

[*] Not available due to a malfunction of the primary detection system.

$M_s = 4160 \pm 100$ A/m. The curve is fitted with a function of the form

$$M(H) = \frac{2}{\pi}\left[\kappa_1 \arctan(\kappa_3 H) + \kappa_2 \arctan(\kappa_4 H)\right], \quad (3)$$

where $\kappa_1 = 1120.25$ A/m, $\kappa_2 = 3103.56$ A/m, $\kappa_3 = 8.49 \cdot 10^{-6}$ m/A, and $\kappa_4 = 1.94 \cdot 10^{-4}$ m/A.

IV. Results and discussion

Estimations for the fundamental axisymmetric and lateral frequencies $\omega_{a/l}$, fundamental damping ratios $\xi_{a/l}$, contact angle θ_c, and lateral hysteresis parameter Γ are obtained after analyzing the laser line projection as described in Sec. III.A. Results are shown in Table 1 as a function of current intensity I for upper and lower containers. Data for the lower container at the 20 A drop is recovered from a time-of-flight sensor. Even though they share the same geometry and a very similar magnetic environment, each container has significantly different values of θ_c (two-sample t-test $t(5) = 3.07$, $p = 0.03$), revealing dissimilar wettability conditions. An analogous bias is observed with Γ, although in this case it is not statistically significant ($t(3) = 0.90$, $p = 0.43$). These effects may be attributed to the potentially uneven application of the hydrophobic treatment over the internal walls of the tanks and to the large sensitivity of water to surface contamination [58, 59].

Microgravity facilities are expensive to operate and their access is generally limited. Having only 4 launch opportunities, the StELIUM team decided to favor the derivation of statistical *trends* rather than statistical *repetitions*. The comparative analysis between individual data points shall thus be treated with care since data dispersion may impair accuracy. Nevertheless, there seems to be a strong dependence between Γ and I when switching between non-magnetic

The final version of this paper can be found in https://doi.org/10.2514/1.J061351

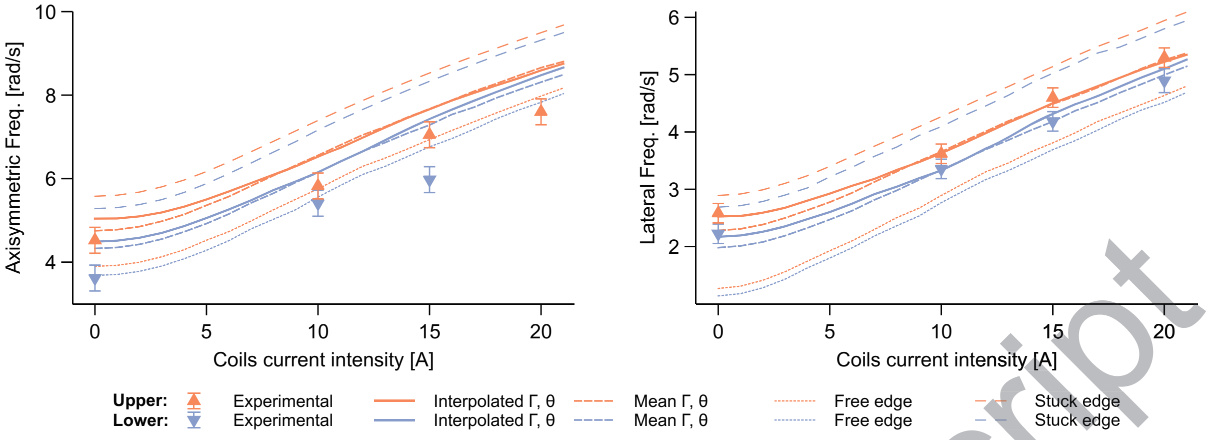

Fig. 3 Axisymmetric (left) and lateral (right) fundamental frequencies as a function of the coils current intensity.

(I = 0 A) and magnetic (I = 10 A) regimes. A 56.3% and 68.0% drop in Γ is observed for upper and lower containers, respectively, suggesting the existence of a shift from surface-tension-dominated to magnetic-force-dominated regimes. To the best knowledge of the authors, this effect has not been reported before and should be confirmed by future studies.

In spite of the aforementioned limitations, solid statistical conclusions can be drawn through the application of appropriate statistics to the variables of interest, as discussed in Ref. 38. Figure 3 shows the fundamental axisymmetric and lateral free surface oscillation frequencies as a function of current intensity. Experimental values, whose error bands are derived by identifying the FFT resolution with the $\pm 3\sigma$ Gaussian interval, are superposed with free edge ($\Gamma = 0$) and stuck edge ($\Gamma \to \infty$) estimations from the model described in Sec. II using mean contact angle values of 62.15° and 52.91° for upper and lower containers, respectively. The use of mean contact angle values is motivated by the absence of a significant linear correlation between I and θ_c for upper ($r(2) = 0.79$, $p = 0.21$) and lower ($r(1) = 0.99$, $p = 0.10$) containers*. From a technical perspective, reducing the number of inputs simplifies the characterization and simulation of the system. The free edge condition is associated with the lowest free surface frequency, while the stuck edge case sets the maximum possible value. Although experimental lateral frequencies fall withing those boundaries, the same does not seem to happen in the axisymmetric case.

Two more theoretical predictions are superposed in Fig. 3: a first one that considers a linear interpolation of the contact angle θ_c and hysteresis Γ values reported in Table 1, and a second that assumes average θ_c and magnetic Γ (upper: 6.25, lower: 5.16) results. Both curves are practically identical, exemplifying the small effect of the contact angle variability, but diverge by ~0.2 rad/s for $I = 0$. This effect is attributed to the large increase of Γ in the non-magnetic case. The most remarkable feature of these predictions is, however, the excellent agreement with experimental results observed for the lateral frequencies. While the interpolation of Γ and θ_c results in an adjusted coefficient of determination

*However, previous works [60–62] have reported a dependence between the apparent contact angle and the applied magnetic field of ferrofluid droplets, an effect that should be explored with larger datasets for the setup employed in this work.

$R^2_{\text{adj}} = 0.983$ (with 3 explanatory variables, Γ, θ_c, and I) and a mean-squared error of $MSE = 0.01$ rad/s, the use of averaged values returns $R^2_{\text{adj}} = 0.976$ with a single explanatory variable I and an $MSE = 0.02$ rad/s. Both models lead to normally distributed residuals according to the Saphiro-Wilk test ($p = 0.075$, $W = 0.84$ and $p = 0.49$, $W = 0.93$ for the fitted and averaged models, respectively). Interestingly, if the frequencies are computed with a restoring inertial acceleration equivalent to the mean magnetic acceleration at the interface (which, for $I = 20$ A, is ~0.71 m/s^2), the deviation at 20 A is just ~0.3 rad/s for both the free and stuck lateral cases. The reasons are that (i) $Bo_{\text{mag}}(R)$ remains almost constant along the meniscus for this setup [38], and (ii) the meniscus profile is only slightly deformed by the magnetic field. In other words, when these two conditions apply, the frequencies can be roughly estimated by assuming a low-gravity interface subject to an equivalent inertial acceleration.

Results for lateral oscillations are in sharp contrast with the axisymmetric case, where the free-edge model ($R^2_{\text{adj}} = 0.873$) performs much better than the rest (e.g. the averaged alternative, $R^2_{\text{adj}} = 0.486$). This is consistent with the analysis reported in Ref. 38, that assumes the free-edge condition, and with the fact that the Γ values are derived from the shape of the lateral sloshing waves. The magnetic response of the model (i.e. its current-frequency slope) cannot be robustly assessed because, unlike in Ref. 38, the small sample size prevents any meaningful comparison. Furthermore, an R^2_{adj} coefficient of just 0.873 is far from acceptable for confirming or denying the conclusions of said reference, where the analytical framework in Sec. II is shown to overestimate the axisymmetric free surface oscillation frequencies. This effect is attributed to unmodeled physical effects, like the potential coupling between Γ and I reported in Tab. 1, that may be addressed in a future work.

The damping ratios reported in Table 1 are computed by means of the half-power bandwidth method as

$$\xi_{a/l} = \frac{1}{2}\frac{\Delta\omega_{-3dB}}{\omega_{a/l}}, \tag{4}$$

where $\Delta\omega_{-3dB}$ is the frequency peak width between the -3 dB points on the FFT spectrum. The division by $\omega_{a/l}$ justifies the decrease of $\xi_{a/l}$ with I. Most importantly, the excellent agreement between inviscid theoretical and experimental lateral frequencies confirms the negligible impact of fluid viscosity and magnetically-induced viscosity [56, 63] on the sloshing problem for the system under study.

From a technical perspective, this analysis shows that, given an educated estimate of θ_c and Γ and an appropriate characterization of the geometric and magnetic environments, the inviscid model first introduced in Ref. 19 and summarized in Sec. II is able to predict the lateral sloshing parameters of a highly-susceptible low-viscosity magnetic liquid in microgravity. This is important for future space applications involving magnetic positive positioning or magnetic liquid sloshing [16] since lateral oscillations represent the largest fuel-induced attitude control disturbance. Furthermore, the results confirm the importance of coupling the magnetic and fluid problems for the study of the dynamics of highly susceptible ferrofluids: if the simplified uncoupled model introduced in Ref. 38 was considered

The final version of this paper can be found in https://doi.org/10.2514/1.J061351

instead, the frequencies at 20 A would be underestimated by 1.37 rad/s and 0.74 rad/s for the axisymmetric and lateral cases, respectively, falling well beyond the error bands. The excellent agreement between experimental results and the averaged model, that operates employing a global estimation of θ_c and Γ, makes basic science discussions on the dependence of such parameters on the applied magnetic field less relevant for most applications, at least for the configuration here considered. The same can be said about axisymmetric oscillations, which have a weaker impact on the spacecraft dynamics [14, 18].

V. Conclusions

The final results of the UNOOSA *DropTES* StELIUM experiment, that studies the axisymmetric and lateral oscillations of a ferrofluid solution in a series of drop tower experiments, validate the quasi-analytical magnetic sloshing model presented in Ref. 19 for the study of lateral oscillations. The small dependence of the contact angle and hysteresis parameter with the applied magnetic field is shown to have an almost negligible impact on the frequency response of the system under study, which simplifies the development of magnetic sloshing control devices. Although the presence of unmodeled physical effects reported in Ref. 38 for the axisymmetric free surface oscillations problem cannot be confirmed due to the small sample size, existing results indicate that the axisymmetric frequencies follow a free-edge behavior rather than the measured lateral hysteresis parameter. The results highlight the importance of accounting for the fluid-magnetic coupling in applications involving highly susceptible ferrofluids.

Competing Interests

The authors declare no competing interests.

Funding Sources

This work was supported by the United Nations Office for Outer Space Affairs (UNOOSA), the Center of Applied Space Technology and Microgravity (ZARM) and the German Space Agency (DLR) in the framework of the UNOOSA DropTES Programme 2019. Further financial and academic support was obtained from Ferrotec Corporation, Politecnico di Milano, the University of Seville, the European Space Agency (ESA) and the European Low Gravity Research Association (ELGRA). A.R.C. acknowledges the financial support offered by the *La Caixa* Foundation (ID 100010434), under agreement LCF/BQ/AA18/11680099.

Acknowledgments

We acknowledge the financial, technical, and academic support offered by UNOOSA, DLR, ZARM, Ferrotec Corporation, Politecnico di Milano, and the University of Seville. We also thank ESA and ELGRA for financing the presentation of this work at the 70th International Astronautical Congress (IAC) and the 26th ELGRA Biennial

Symposium and General Assembly. We are in debt with ZARM's drop tower engineers Jan Siemer and Fred Oetken, ZARM's point of contact Dr Thorben Könemann and UNOOSA's point of contact Ayami Kojima for their endless support. We would like to thank the technicians Giovanni Colombo, Alberto Verga and the PhD student Riccardo Bisin from the Space Propulsion Laboratory (SPLab) of Politecnico di Milano for their academic and technical assistance, as well as the rest of members of this research group for contributing to the creation of an extraordinary professional and human environment. Finally, we acknowledge the support offered by Prof. Elena Castro-Hernández, Prof. Gabriel Cano-Gómez, and Prof. Miguel Herrada in the early stages of the StELIUM project.

References

[1] Wakayama, N. I., "Magnetic buoyancy force acting on bubbles in nonconducting and diamagnetic fluids under microgravity," *Journal of Applied Physics*, Vol. 81, No. 7, 1997, pp. 2980–2984. https://doi.org/10.1063/1.364330.

[2] Wakayama, N. I., "Utilization of magnetic force in space experiments," *Advances in Space Research*, Vol. 24, No. 10, 1999, pp. 1337 – 1340. https://doi.org/10.1016/S0273-1177(99)00743-7, gravitational Effects in Materials and Fluid Sciences.

[3] Boulware, J. C., Ban, H., Jensen, S., and Wassom, S., "Experimental studies of the pressures generated by a liquid oxygen slug in a magnetic field," *Journal of Magnetism and Magnetic Materials*, Vol. 322, No. 13, 2010, pp. 1752 – 1757. https://doi.org/10.1016/j.jmmm.2009.12.022.

[4] Kinefuchi, K., and Kobayashi, H., "Theoretical and experimental study of the active control of bubble point pressure using a magnetic field and its applications," *Physics of Fluids*, Vol. 30, No. 6, 2018, p. 062101. https://doi.org/10.1063/1.5034222.

[5] Causevica, A., Sahli, P., Hild, F., Grunwald, K., Ehresmann, M., and Herdrich, G., "PAPELL: Interaction Study of Ferrofluid with Electromagnets of an Experiment on the International Space Station," *Proceedings of the 69th International Astronautical Congress*, 2018, pp. 1–5.

[6] Jackson, B. A., Terhune, K. J., and King, L. B., "Ionic liquid ferrofluid interface deformation and spray onset under electric and magnetic stresses," *Physics of Fluids*, Vol. 29, No. 6, 2017, p. 064105. https://doi.org/10.1063/1.4985141.

[7] Lemmer, K., "Propulsion for CubeSats," *Acta Astronautica*, Vol. 134, 2017, pp. 231 – 243. https://doi.org/10.1016/j.actaastro.2017.01.048.

[8] Hild, F., Ehresmann, M., and Herdrich, G., "Concept Design of an in-Orbit Propulsion System based on Magnetofluids," *Proceedings of the 71st International Astronautical Congress (IAC)*, 2020.

[9] Ludovisi, D., Cha, S. S., Ramachandran, N., and Worek, W. M., "Heat transfer of thermocapillary convection in a two-layered fluid system under the influence of magnetic field," *Acta Astronautica*, Vol. 64, No. 11, 2009, pp. 1066 – 1079. https://doi.org/10.1016/j.actaastro.2009.01.018.

[10] Bozhko, A., and Putin, G., "Thermomagnetic Convection as a Tool for Heat and Mass Transfer Control in Nanosize Materials Under Microgravity Conditions," *Microgravity Science and Technology*, Vol. 21, No. 1, 2009, pp. 89–93. https://doi.org/10.1007/s12217-008-9059-7.

[11] Scarl, E., and Houston, J., "Two-phase magnetic fluid manipulation in microgravity environments," *Proceedings of the 37th Aerospace Sciences Meeting and Exhibit*, 1999, pp. 1–5. https://doi.org/10.2514/6.1999-844.

[12] Tillotson, B. J., Torre, L. P., and Houston, J. D., "Method for Manipulation of Diamagnetic Objects in a Low-Gravity Environment," , 2000. US Patent 6162364.

[13] Romero-Calvo, A., Cano-Gómez, G., and Schaub, H., "Diamagnetically Enhanced Electrolysis and Phase Separation in Low Gravity," *Journal of Spacecraft and Rockets*, 2021. https://doi.org/10.2514/1.A35021, *in press*.

[14] Dodge, F., *The New Dynamic Behavior of Liquids in Moving Containers*, Southwest Research Institute, 2000.

[15] Álvaro Romero-Calvo, Cano-Gómez, G., Hermans, T. H., Parrilla Benítez, L., Ángel Herrada Gutiérrez, M., and Castro-Hernández, E., "Total magnetic force on a ferrofluid droplet in microgravity," *Experimental Thermal and Fluid Science*, Vol. 117, 2020, pp. 110–124. https://doi.org/10.1016/j.expthermflusci.2020.110124.

[16] Romero-Calvo, A., Maggi, F., and Schaub, H., "Magnetic Positive Positioning: Toward the application in space propulsion," *Acta Astronautica*, Vol. 187, 2021, pp. 348–361. https://doi.org/10.1016/j.actaastro.2021.06.045.

[17] Myshkis, A., Babskii, V., Kopachevskii, N., Slobozhanin, L., and Tyuptsov, A., *Low-gravity fluid mechanics: mathematical theory of capillary phenomena*, Springer, 1987.

[18] Reynolds, W. C., and Satterlee, H. M., *The Dynamic Behavior of Liquids in Moving Containers*, NASA SP-106, 1966.

[19] Romero-Calvo, A., Cano Gómez, G., Castro-Hernández, E., and Maggi, F., "Free and forced oscillations of magnetic liquids under low-gravity conditions," *Journal of Applied Mechanics*, Vol. 87, No. 2, 2020. https://doi.org/10.1115/1.4045620, 021010.

[20] Baozeng, Y., Wenjun, W., and Yulong, Y., "Modeling and Coupling Dynamics of the Spacecraft with Multiple Propellant Tanks," *AIAA Journal*, Vol. 54, No. 11, 2016, pp. 3608–3618. https://doi.org/10.2514/1.J055110.

[21] Utsumi, M., "Slosh Damping Caused by Friction Work Due to Contact Angle Hysteresis," *AIAA Journal*, Vol. 55, No. 1, 2017, pp. 265–273. https://doi.org/10.2514/1.J055238.

[22] Yulong, Y., and Baozeng, Y., "Dynamic Analysis of the Flexible Spacecraft with Liquid Sloshing in Axisymmetrical Container," *Journal of Spacecraft and Rockets*, Vol. 55, No. 2, 2018, pp. 282–291. https://doi.org/10.2514/1.A34005.

[23] Dong, H., Liu, S., Wu, W., and Liu, Z., "Mode Shape Experimental Characterization Technique of Liquid Sloshing in a Complex-Shaped Tank," *AIAA Journal*, Vol. 57, No. 4, 2019, pp. 1773–1780. https://doi.org/10.2514/1.J057821.

[24] Navabi, M., Davoodi, A., and Reyhanoglu, M., "Modeling and control of a nonlinear coupled spacecraft-fuel system," *Acta Astronautica*, Vol. 162, 2019, pp. 436–446. https://doi.org/10.1016/j.actaastro.2019.06.029.

[25] Yu, Q., Wang, T., and Li, Z., "Rapid Simulation of 3D Liquid Sloshing in the Lunar Soft-Landing Spacecraft," *AIAA Journal*, Vol. 57, No. 10, 2019, pp. 4504–4513. https://doi.org/10.2514/1.J058160.

[26] Feng, L., Baozeng, Y., Banerjee, A. K., Yong, T., Wenjun, W., and Zhengyong, L., "Large Motion Dynamics of In-Orbit Flexible Spacecraft with Large-Amplitude Propellant Slosh," *Journal of Guidance, Control, and Dynamics*, Vol. 43, No. 3, 2020, pp. 438–450. https://doi.org/10.2514/1.G004685.

[27] Martin, J., and Holt, J., "Magnetically Actuated Propellant Orientation Experiment, Controlling fluid Motion With Magnetic Fields in a Low-Gravity Environment," Tech. Rep. TM-2000-210129, M-975, NAS 1.15:210129, NASA, 2000.

[28] Hochstein, J., R. Warren, J., George Schmidt, J., Hochstein, J., R. Warren, J., and George Schmidt, J., "Magnetically Actuated Propellant Orientation (MAPO) Experiment - Pre-flight flow field predictions," *35th Aerospace Sciences Meeting and Exhibit*, 1997. https://doi.org/10.2514/6.1997-570, AIAA Paper 97-0570.

[29] Marchetta, J., and Hochstein, J., "Fluid capture by a permanent ring magnet in reduced gravity," *Proceedings of the 37th Aerospace Sciences Meeting and Exhibit, Reno, NV, USA*, American Institute of Aeronautics and Astronautics, 1999. https://doi.org/10.2514/6.1999-845, AIAA Paper 99-0845.

[30] Marchetta, J., and Hochstein, J., "Simulation and dimensionless modeling of magnetically induced reorientation," *Proceedings of the 38th Aerospace Sciences Meeting and Exhibit, Reno, NV, USA*, American Institute of Aeronautics and Astronautics, 2000. https://doi.org/10.2514/6.2000-700, AIAA Paper 2000-0700.

[31] Marchetta, J., Hochstein, J., Sauter, D., and Simmons, B., "Modeling and prediction of magnetic storage and reorientation of LOX in reduced gravity," *40th AIAA Aerospace Sciences Meeting & Exhibit*, American Institute of Aeronautics and Astronautics, 2002. https://doi.org/10.2514/6.2002-1005, AIAA Paper 2002-1005.

[32] Marchetta, J. G., "Simulation of LOX reorientation using magnetic positive positioning," *Microgravity - Science and Technology*, Vol. 18, No. 1, 2006, p. 31. https://doi.org/10.1007/BF02908417.

[33] Marchetta, J., and Roos, K., "A Three-Dimensional Computational Simulation of Magnetic Positive Positioning," *45th AIAA Aerospace Sciences Meeting and Exhibit, Reno, Nevada*, 2007. https://doi.org/10.2514/6.2007-956, AIAA Paper 2007-956.

[34] Marchetta, J., and Roos, K., "Simulating Magnetic Positive Positioning of Liquids in a Transient Acceleration Field," *46th AIAA Aerospace Sciences Meeting and Exhibit, Reno, Nevada*, 2008. https://doi.org/10.2514/6.2008-820, AIAA Paper 2008-820.

[35] Marchetta, J., and Winter, A., "Simulation of magnetic positive positioning for space based fluid management systems," *Mathematical and Computer Modelling*, Vol. 51, No. 9, 2010, pp. 1202 – 1212. https://doi.org/10.1016/j.mcm.2010.01.002.

[36] Romero-Calvo, A., Hermans, T., Cano Gómez, G., Parrilla Benítez, L., Herrada Gutiérrez, M. A., and Castro-Hernández, E., "Ferrofluid Dynamics in Microgravity Conditions," *Proceedings of the 2nd Symposion on Space Educational Activities*, 2018.

[37] Romero-Calvo, A., Hermans, T., Parrilla Benítez, L., and Castro-Hernández, E., "Drop Your Thesis! 2017 Experiment Report - Ferrofluid Dynamics in Microgravity Conditions," Tech. rep., ESA, 2018.

[38] Romero-Calvo, Á., Herrada, M. Á., Hermans, T. H. J., Benítez, L. P., Cano-Gómez, G., and Castro-Hernández, E., "Axisymmetric Ferrofluid Oscillations in a Cylindrical Tank in Microgravity," *Microgravity Science and Technology*, Vol. 33, No. 4, 2021, p. 50. https://doi.org/10.1007/s12217-021-09894-4.

[39] Romero-Calvo, A., García-Salcedo, A., Garrone, F., Rivoalen, I., Cano-Gómez, G., Castro-Hernández, E., Gutiérrez, M. H., and Maggi, F., "StELIUM: A student experiment to investigate the sloshing of magnetic liquids in microgravity," *Acta Astronautica*, Vol. 173, 2020, pp. 344 – 355. https://doi.org/10.1016/j.actaastro.2020.04.013.

[40] Romero-Calvo, A., García-Salcedo, A., Garrone, F., Rivoalen, I., Cano-Gómez, G., Castro-Hernández, E., and Maggi, F., "Free surface reconstruction of opaque liquids in microgravity, Part 1: Design and on-ground testing," *Acta Astronautica*, Vol. 189, 2021, pp. 250–259. https://doi.org/10.1016/j.actaastro.2021.08.029.

[41] Romero-Calvo, A., Garrone, F., García-Salcedo, A., Rivoalen, I., Cano-Gómez, G., Castro-Hernández, E., and Maggi, F., "Free surface reconstruction of opaque liquids in microgravity. Part 2: Drop tower campaign," *Acta Astronautica*, Vol. 189, 2021, pp. 269–277. https://doi.org/10.1016/j.actaastro.2021.07.020.

[42] Bauer, H. F., "Liquid Sloshing in a Cylindrical Quarter Tank," *AIAA Journal*, Vol. 1, No. 11, 1963, pp. 2601–2606. https://doi.org/10.2514/3.2118.

[43] Yeh, G. C. K., "Free and Forced Oscillations of a Liquid in an Axisymmetric Tank at Low-Gravity Environments," *Journal of Applied Mechanics*, Vol. 34, No. 1, 1967, pp. 23–28. https://doi.org/10.1115/1.4045620.

[44] Dodge, F. T., and Garza, L. R., "Experimental and Theoretical Studies of Liquid Sloshing at Simulated Low Gravities," Tech. Rep. CR-80471, NASA, 1969.

[45] P. Concus, G. C., and Satterlee, H., "Small amplitude lateral sloshing in a cylindrical tank with a hemispherical bottom under low gravitational conditions," Tech. Rep. CR-54700, LMSC-A852007, NASA, January 1967.

[46] P. Concus, G. C., and Satterlee, H., "Small amplitude lateral sloshing in spheroidal containers under low gravitational conditions," Tech. Rep. CR-72500, LMSC-A944673, NASA, 1969.

[47] Salzman, J. A., and Masica, W. J., "Lateral Sloshing in Cylinders Under Low-Gravity Conditions," Tech. Rep. TN D-5058, NASA, 1969.

[48] Dodge, F. T., and Garza, L. R., "Simulated low-gravity sloshing in spherical, ellipsoidal, and cylindrical tanks," *Journal of Spacecraft and Rockets*, Vol. 7, No. 2, 1970, pp. 204–206. https://doi.org/10.2514/3.29900.

[49] Dodge, F. T., "Further Studies of Propellant Sloshing Under Low-Gravity Conditions," Tech. Rep. CR-11989, NASA, 1971.

[50] Coney, T., and Salzman, J., "Lateral sloshing in oblate spheroidal tanks under reduced- and normal-gravity conditions," Tech. Rep. TN D-6250, NASA, 1971.

[51] Concus, P., and Crane, G. E., "Discussion: "Free and forced oscillations of a liquid in an axisymmetric tank at low-gravity evironments" (Yeh, Gordon C. K., 1967, ASME J. Appl. Mech., 34, pp. 23-28)," *Journal of Applied Mechanics*, Vol. 34, No. 4, 1967, pp. 1051–1052.

[52] Chu, W.-H., "Low-Gravity Fuel Sloshing in an Arbitrary Axisymmetric Rigid Tank," *Journal of Applied Mechanics*, Vol. 37, No. 3, 1970, pp. 828–837. https://doi.org/10.1115/1.3408616.

[53] Satterlee, H. M., and Reynolds, W. C., "The Dynamics of Free Liquid Surface in Cylindrical Containers Under Strong Capillary and Weak Gravity Conditions," Tech. Rep. LG-2, Stanford University Mechanical Engineering Department, 1964.

[54] Abramson, H. N., Chu, W.-H., and Garza, L. R., "Liquid Sloshing in Spherical Tanks," *AIAA Journal*, Vol. 1, No. 2, 1963, pp. 384–389. https://doi.org/10.2514/3.1542.

[55] Bauer, H. F., "Nonlinear Mechanical Model for the Description of Propellant Sloshing," *AIAA Journal*, Vol. 4, No. 9, 1966, pp. 1662–1668. https://doi.org/10.2514/3.3752.

[56] Rosensweig, R. E., *Ferrohydrodynamics*, Dover Publications, 1997.

[57] ZARM, *ZARM Drop Tower User Manual*, ZARM FABmbH, 2011. Drop Tower Operation and Service Company.

[58] Nicolás, J. A., and Vega, J. M., "A note on the effect of surface contamination in water wave damping," *Journal of Fluid Mechanics*, Vol. 410, 2000, pp. 367–373. https://doi.org/10.1017/S002211209900823X.

[59] Herrada, M. A., Montanero, J. M., and Vega, J. M., "The effect of surface shear viscosity on the damping of oscillations in millimetric liquid bridges," *Physics of Fluids*, Vol. 23, No. 8, 2011, p. 082102. https://doi.org/10.1063/1.3623425.

[60] Rigoni, C., Pierno, M., Mistura, G., Talbot, D., Massart, R., Bacri, J.-C., and Abou-Hassan, A., "Static Magnetowetting of Ferrofluid Drops," *Langmuir*, Vol. 32, No. 30, 2016, pp. 7639–7646. https://doi.org/10.1021/acs.langmuir.6b01934.

[61] Souza, P., Lira, S., and de Oliveira, I., "Wetting dynamics of ferrofluids on substrates with different hydrophilicity behaviors," *Journal of Magnetism and Magnetic Materials*, Vol. 483, 2019, pp. 129 – 135. https://doi.org/10.1016/j.jmmm.2019.03.069.

[62] Guba, S., Horváth, B., and Szalai, I., "Examination of contact angles of magnetic fluid droplets on different surfaces in uniform magnetic field," *Journal of Magnetism and Magnetic Materials*, Vol. 498, 2020, p. 166181. https://doi.org/10.1016/j.jmmm.2019.166181.

[63] Shliomis, M., "Effective Viscosity of Magnetic Suspensions," *Soviet Physics JETP*, Vol. 34, 1972, pp. 1291–1294.